Price Inflation Effects on a Solar-Geothermal System for Combined Production of Hydrogen, Power, Freshwater and Heat

Ali Sohani [a], Fatemeh Delfani [b], Mohammadmehdi Hosseini [a], Hoseyn Sayyaadi [a], Nader Karimi [c, d], Larry K.B. Li [e], Mohammad Hossein Doranehgard [e, f 1]

[a] Lab of Optimization of Thermal Systems' Installations, Faculty of Mechanical Engineering-Energy Division, K.N. Toosi University of Technology, P.O. Box: 19395-1999, No. 15-19, Pardis St., Mollasadra Ave., Vanak Sq., Tehran 1999 143344, Iran

[b] Department of Mechanical Engineering, Semnan Branch, Islamic Azad University, Semnan, Iran

[c] School of Engineering and Materials Science, Queen Mary University of London, London E1 4NS, United Kingdom

[d] James Watt School of Engineering, University of Glasgow, Glasgow G12 8QQ, United Kingdom

[e] Department of Mechanical and Aerospace Engineering, Hong Kong University of Science and Technology, Clear Water Bay, Hong Kong

[f] Department of Civil and Environmental Engineering, School of Mining and Petroleum Engineering, University of Alberta, Edmonton, Alberta T6G 1H9, Canada

Abstract

This study explores the effects of price inflation on the optimal performance of a solar-geothermal system capable of combined production of hydrogen, power, freshwater and heat. Multi-objective optimization is applied, with the ground water mass flow rate and the solar collector area as the decision variables, alongside the payback period and the annual production of hydrogen, power, freshwater and heat as the objective functions. The results show that when inflation rises four-fold

[1] Corresponding author; Email address: doranehg@ualberta.ca (M.H. Doranehgard).

from 0.05 to 0.20, the ground water mass flow rate drops by 20.1%, while the solar collector area rises by 14.4%. Accompanying this are 15.0%, 12.2% and 12.0% decreases in annual freshwater, power and heat production, respectively, alongside a 9.9% increase in annual hydrogen production. The payback period, meanwhile, increases only modestly, from 6.11 to 7.39 years, demonstrating the economic viability of such a combined solar-geothermal system, even in inflationary times.

Keywords: Clean hydrogen production; Desalination; Economic analysis; Optimum performance; Poly-generation.

Nomenclature

Symbols

a	Pairwise matrix element
r	Normalized weight of the pairwise comparison matrix
s	Summation of the rows of the pairwise comparison matrix
w	Weight in the pairwise comparison of AHP
W	Final weight of an alternative in AHP

Subscripts

i	Pairwise matrix i^{th} row
j	Pairwise matrix j^{th} column

Abbreviations

AHP	Analytical hierarchy process
TOPSIS	Technique for order preferences based on the similarity to the ideal solution
TES	Thermal energy storage
MED	Multi-effect desalination
CSP	Concentrated solar power
NSGA-II	Non-dominated sorting genetic algorithm II
PTC	Parabolic trough collector

1. Introduction

For over a century, global energy demand has risen to support increased urbanization, enhanced quality of life, and socio-economic development [1-3]. Previously this demand has been met primarily through the combustion of fossil-based energy resources, but this is now known to be a major contributor to greenhouse gas emissions and climate change, posing serious threats to our ecosystem and human civilization [4]. According to the IEA, global energy demand is expected to rise by more than 4% in 2022, an increase that is to be partly met by fossil-based energy resources,

especially in underdeveloped nations [5]. At the 2021 United Nations Climate Change Conference (COP26) held in Scotland, the global community could only agree to "phase-down" (rather than "phase-out") the use of coal, highlighting the need to develop more sustainable but economically viable alternatives for energy production and conversion [6-8].

Renewable energy systems are a promising alternative to fossil-based technologies [9-11]. Some systems of this sort can also produce heat, hydrogen, and water to meet societal needs [12-14]. The efficient production and management of renewable energy would not only reduce our overall carbon intensity, but it would also reduce our reliance on fossil fuels, contributing to environmental sustainability while meeting the energy, security, and water challenges of our societies [15]. In this context, poly-generation technologies powered by renewable energy offer profound potential [16]. They can enhance the utilization of natural resources while promoting energy efficiency and reducing costs, both monetary and environmental [16].

In a poly-generation system, multiple objectives – such as the production of power, cooling, heating, hydrogen gas, and water – are simultaneously realized through integrated processes driven by various energy resources, including those with renewable credentials such as solar and geothermal [17]. There is a need to carefully analyze such integrated processes to estimate their energy efficiency and production performance. Sen et al. [18] have conducted thermodynamic modeling and analysis for electricity and hydrogen production from a multi-generation system powered by geothermal and solar resources. The overall exergy and energy efficiency values were estimated 18.99% and 5.90%. Analysis based on exergy and energy perspectives was performed on a concentrated photovoltaic recupaerator for a geothermal poly-generation system, where a noticeable performance improvement was found [19]. Siddiqui et al. analyzed an innovative multi-

generation unit powered by solar and geothermal energy. The exergy and energy efficiencies were found to be up to 19.1% and 19.6%, respectively [20].

Multi-objective optimization can be used to find optimal solutions even with competing objectives. Chitgar et al. [21] proposed an integrated GT-SOFC system to generate electricity, freshwater, and H_2. The system was optimized using a genetic algorithm combined with multi-objective optimization, and the optimal solutions for various built-in scenarios were found. Ebrahimi–Moghadam et al. [22] presented optimal solutions for the simultaneous production of electricity, heating, and cooling, and hydrogen from a multi-generation district heating system. Alirahmi et al. [23, 24] reported the simultaneous production of electricity, hydrogen, heating and cooling using thermodynamic modeling and multi-objective design optimization. Other studies have analyzed solar multi-generation systems using multi-objective optimization [25, 26].

Location selection is critical when installing a poly-generation system, because the availability of resources and energy potential varies around the world. Mostafaeipour et al. [27] performed an econometric analysis to produce electricity and hydrogen gas from the available wind potential in four Iranian cities. A minimum payback period of 5 years was found for a 100 kW wind turbine installed at Ardebil. Various decision-making and planning techniques were used to identify the best site location and to estimate the wind/solar potential to produce hydrogen and electricity [28-32].

Turning to techno-economic assessments, Li et al. [33] performed thermal modeling, economic analysis, and optimization on a geothermal tri-generation unit producing water, hydrogen, and power. A payback period of up to 2.385 years was found when optimizing the three objectives. Shaofu et al. [34] conducted thermo-economic and optimization analyses for hydrogen production using waste heat from a steel plant.

Safari and Dincer [35] applied exergoenvironmental and exergoeconomic analyses, based on the first and second laws of thermodynamics, to a cogeneration system in which a vanadium-chlorine (V-Cl) thermochemical cycle was utilized for hydrogen production. It was found that the optimized environmental impact value, exergy efficiency, and total cost per unit of exergy were 14.46 $g.CO_2.(kWh)^{-1}$, 60.45%, and 6.36 $\$.(GJ)^{-1}$ respectively. Using an exergoeconomic analysis and the SPECO method to assess the exergy cost, Farsi et al. [36] experimentally investigated a copper-chlorine (Cu-Cl) cycle for hydrogen generation. They found that producing hydrogen from a Cu-Cl plant with a capacity of 1000 kg of H_2 per day would cost \$3.91 per kg of H_2.

Ansari et al. [37] presented a comprehensive investigation of the energetic and exergetic performance of a multigeneration system used for space heating, space cooling, electric power, hot water, freshwater and hydrogen provision. The exergy efficiency of the system was 67.9%, while the energy efficiency was 49.1%. Moreover, Mahmoudan et al. [38] applied multi-objective optimization to a multi-generation system in order to minimize its total cost, as well as maximizing its exergy efficiency. The results showed that, when the system is operated at its optimized condition, the total unit cost of the products, exergy efficiency and hydrogen production rate are 37.8 $\$.(GJ)^{-1}$, 35.2%, and 1.9 $kg.h^{-1}$, respectively.

A concentrated solar-geothermal poly-generation system − producing hydrogen, space heating, freshwater and electricity − was proposed by Temiz and Dincer [2]. The system featured a geothermal unit, a thermochemical Cu-Cl H_2 production unit, a trilateral ammonia Rankine cycle power generation unit, a desalination unit, a residential heat pump, and concentrated solar power assisted by thermal energy storage. Space heating, freshwater, and electricity requirements were met via geothermal energy. Sensitivity analysis performed at the component level, as well as energy, exergy and cost analyses for the whole unit and at the component level were performed.

The H_2 and electricity production costs were estimated at $2.84 per kg and $0.03 per kWh, respectively. At ambient conditions for the case-study location (Geysers, California, USA), the exergy and energy efficiencies were 17.3% and 27.4%, respectively. These results indicated that the system could represent an efficient and economical choice. A multi-objective optimization approach was adopted by Sohani et al. [39] for the system proposed in Ref. [2]. The results showed that the payback period dropped from 5.6 to 4.4 years, with considerable improvements in system productivity and efficiency. In that study, however, a single rate of price inflation was assumed. NSGA-II and TOPSIS were adopted in selecting the optimal solution.

From the above literature review, two research gaps can be identified in the optimization of multi-generation systems to produce hydrogen:

- In most studies, only a single rate of price inflation was assumed. In other words, the effect of rising inflation on multi-objective optimization of multi-generation systems has yet to be systematically investigated.

- The optimal solution was identified via TOPSIS or other decision-making approaches, in which the importance of all the objective functions is assumed to be the same. However, in real-world scenarios, some criteria are often more important than others. To the best of our knowledge, in the analysis of complex multi-generation systems, advanced decision-making methods − such as those involving analytical hierarchy processes (AHPs), which consider the relative importance of different criteria − have been used only to identify the ideal location at which to install such systems, not to optimize the system processes themselves.

In the present study, we consider the combined production of hydrogen, power, freshwater and heat via multi-objective optimization.

- The effects of price inflation on the multi-objective optimization are examined. For the solar-geothermal system under consideration, the effects of inflation on the optimal values of the solar collector area and the extracted ground water flow rate are examined. Also examined are the effects of inflation on the optimum values of the objective functions, namely the production of hydrogen, power, freshwater, and heat during a year, as well as the payback period. This is the primary novelty of this study. It is worth noting that although the impact of price inflation on the optimization results has been studied for some energy systems like coolers [40] and solar stills [41], it has not been studied for more complex multi-generation systems, such as that examined in the present study.

- Here AHP is used instead of TOPSIS to converge to the final optimal solution. In this way, the relative importance of the objective functions is accounted for, providing more realistic conditions for multi-objective optimization. This is the secondary novelty of this study.

2. Methodology

The system under study is described first, followed by a presentation of the multi-objective optimization procedure and a representative case study.

2.1. The investigated multi-generation system

Figure 1 introduces the investigated multi-generation system. The system combines a Cu-Cl cycle with renewable energy assisted technologies to produce power, heat, H_2 and freshwater. The subsystems consist of a PTC, a CSP, a TES, a geothermal source, a Cu-Cl thermochemical H_2 generation unit, a trilateral ammonia Rankine cycle electricity production unit, an MED system

and a residential heat pump. It requires a high-grade heat source, possibly at around 550°C, to ensure feasible and reliable Cu-Cl thermochemical H_2 production. For this, a parabolic trough solar collector is installed at the site. A temperature higher than 120°C is needed for geothermal energy, and an annual global horizontal irradiation of greater than 1500 $kWh.m^{-2}$ is required for solar energy.

Geothermal energy is used for the auxiliary Cu-Cl system. The system is installed in a closed loop, with a reinjection system in place to avoid chemical and thermal pollution. The heat source comes from a trilateral ammonia Rankine cycle, which runs with geothermal power. The excess heat from this cycle is dissipated to a R-134a heat pump. The required heat for space heating is supplied by the heat pump at 60°C. Steam at 76°C and 0.4 bar from a separator enters the MED system to produce freshwater from salty water. Another heat exchanger is fed by the separator remaining ground water for heating around the year. Geothermal water is discharged to a well after passing through a mixing chamber. The solar side of the multi-generation unit also provides heat for a Cu-Cl thermochemical chamber to produce hydrogen gas in four steps: hydrolysis, thermolysis, electrolysis, and drying. The hydrogen undergoes compression and other processes, becoming hydrogen fuel for vehicles. The electrical load is supplied by the geothermal source, whereas the heating load is supplied by TES and CSP parts. The full specifications of the system can be found in Ref. [2].

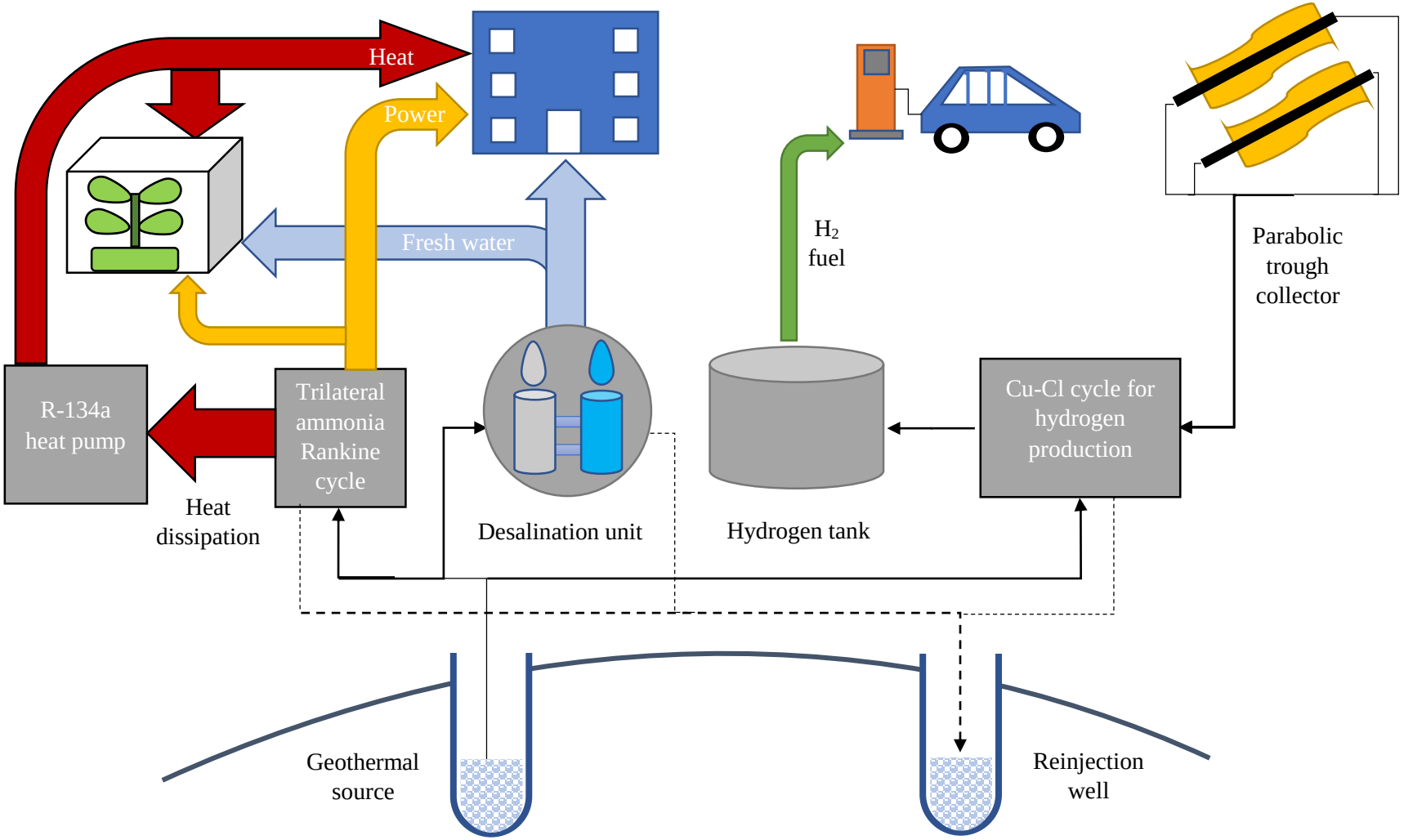

Figure 1. Schematic diagram of the investigated system

2.2. Multi-objective optimization

Here NSGA-II and AHP are combined for multi-objective optimization. Because the details of this procedure have been described previously (see Refs. [42] and [43]), only a brief overview is given here. The optimization is performed for the following parameters:

$$\begin{cases} \max & \textit{Annual } H_2 \textit{ production} \\ \max & \textit{Annual electricity production} \\ \max & \textit{Annual fresh water production} \\ \max & \textit{Annual heat production} \\ \min & \textit{Payback period} \end{cases} \quad (1)$$

The solar collector area and the extracted ground water mass flow rate are the decision variables, with no constraints imposed. As the modeling approach here is the same as that in Ref. [2], the reader is referred to that reference for details regarding the modeling. In the present study, NSGA-II and AHP are used to determine the number of candidate solutions and the best solution, respectively. These techniques are used because of their performance relative to other available methods [43].

2.2.1. NSGA-II

NSGA-II is a method of determining a set of solutions that has the potential of being the optimal solution. Its working principle can be described as follows:

1. First, a set of answers is generated randomly, producing an initial population.
2. Each solution is compared with the others. If the optimization goal is to minimize all the objectives, answer ‘A’ dominates answer ‘B’ if:

   2.1. Each element of ‘A’ is smaller than or equal to the corresponding element of ‘B’.

2.2. ‘B’ has at least one strictly larger element.

3. The dominancy degree, which is the number of answers dominating a solution, is calculated for each answer.

4. Answers are listed according to the dominancy degree, with solutions of the same dominancy degree forming a group.

5. The process to generate the next population begins. If the number of solutions in each group is lower than the number of the required answers, all of them are chosen. Otherwise, the answers in each group are listed according to a parameter called the crowding distance, and the solution with the larger crowding distance is selected until the required number of solutions is reached for the next generation.

6. Answers with the lowest dominancy degree are grouped together to form the Pareto optimal frontier (POF).

   6.1. If one of the stopping criteria is met, the POF is introduced as the output of NSGA-II.

   6.2.Otherwise, the next generation is formed, and the process is repeated via step 2.

2.2.2. Analytic hierarchy process

In engineering applications, decision making methods are often used to converge to the best answers on the POF. This is usually done via methods such as TOPSIS and LINMAP. However, as noted earlier, such methods do not account for any priority of the objective functions when identifying the optimal point, while AHP considers different degrees of importance for each objective function. Consequently, AHP is used here as the decision making method to achieve a more representative outcome from multi-objective optimization. This method, developed by Saaty

[44], is based on pairwise comparisons of the criteria when choosing the final optimized solution. It contains several stages:

1. First, the important criteria for choosing the best alternative are introduced.
2. If there are any subcriteria, they are defined as well.
3. The degree of importance is specified, with three comparison levels [44]:

   3.1. Alternatives with respect to each subcriterion (if any). If there are no subcriteria for a criterion, comparing the alternatives is done directly with respect to that criterion.

   3.2. Subcriteria with respect to each criterion, if there are subcriteria for a criterion.

   3.3. Criteria with respect to the main goal of the decision making.

   The importance degree of C to D is represented by w_{CD} , and the importance degree of D to C is represented by w_{DC} , which is simply $\frac{1}{w_{CD}}$.

4. For each alternative, the preference index is computed. The final point is the one with the highest preference index. The pairwise comparison matrix is:

$$A = \begin{bmatrix} 1 & a_{12} & \dots & a_{1n} \\ a_{21} & 1 & \dots & a_{2n} \\ \vdots & \vdots & \ddots & \vdots \\ a_{n1} & a_{n2} & \dots & 1 \end{bmatrix} \quad (2)$$

To obtain the weight (w), the following steps are followed:

4.1. Find the summation of each column:

$$s_i = \sum_{j=1}^{n} a_{ij} \quad i = 1, 2, ..., n \tag{3}$$

4.2.Normalize the elements of the matrix A:

$$r_{ij}^{normal} = \frac{a_{ij}}{s_i} \tag{4}$$

4.3. Determine the weight of each element:

$$w_i = \frac{\sum_{i=1}^{n} r_{ij}^{normal}}{n} \tag{5}$$

4.4. The local weights are determined for each alternative, and then the preference index is determined:

$$W_i = \sum_{j=1}^{m} w_{ij} \times w_j \tag{6}$$

The weight of the ith solution with respect to the jth criterion is given by w_{ij} . w_j also represents the weight of the jth criterion.

Determining the weights of the pairwise comparison matrix can be challenging because there might be competition among the experts. In such scenarios, the geometric mean of the given weight from each expert is used, as per [45].

2.3. A representative case study

Tehran, the capital and largest city in Iran, is selected as the focus of our case study. It has a population of over 10 million. Damavand, a region in the northeastern part of the city, is chosen as the site for system installation. This region is at a latitude of 35.70°N and a longitude of 52.06°E. It receives abundant solar radiation and has a high ground temperature.

Iran is facing severe water scarcity. Therefore, among the objective functions, the annual freshwater production is given the highest priority. After that, and because of persistent power shortages in the country, the annual electricity production is given the second highest priority. These two objective functions are followed by the payback period. Because the country has vast deposits of natural gas and oil, and because high subsidies are applied to vehicular fuels, the annual production of heat and hydrogen are prioritized fourth and fifth, respectively. Table (1) lists the priority in the form of a pairwise comparison matrix.

Table (1): Matrix of pairwise comparison for the objective functions, which are the decision criteria of AHP.

	Annual freshwater	Annual power	Annual H_2 production	Annual heat	Payback period
Annual freshwater	1	2	6	5	3
Annual power	$\frac{1}{2}$	1	3	4	2
Annual H_2 production	$\frac{1}{6}$	$\frac{1}{3}$	1	$\frac{1}{2}$	$\frac{1}{2}$
Annual heat	$\frac{1}{5}$	$\frac{1}{4}$	2	1	$\frac{1}{3}$
Payback period	$\frac{1}{3}$	$\frac{1}{2}$	2	3	1

The ranges of the two decision variables are as follows:

- 0 to 200,000 m^2 for the solar collector area.
- 0 to 5,000 $kg.s^{-1}$ for the extracted ground water mass flow rate.

3. Results and discussion

This part gives the results from the numerical simulations. The results are first validated, and then the effect of price inflation on the optimal design and performance of the system is examined.

3.1. Validation of the modeling framework

The results of Ref. [2] are used for system validation. Figure 2 shows that there are only minor differences between the data of Ref. [2] and the simulation data of the present study. For example, errors of 1.31% and 0.81% are found in January and July, respectively. The mean and maximum errors are 1.16% and 1.72%, respectively, demonstrating the reliability of the present numerical framework. It is worth noting that as the data from Ref. [2] is for the city Geysers, California, USA, the simulation data shown here is for this region as well, ensuring consistency.

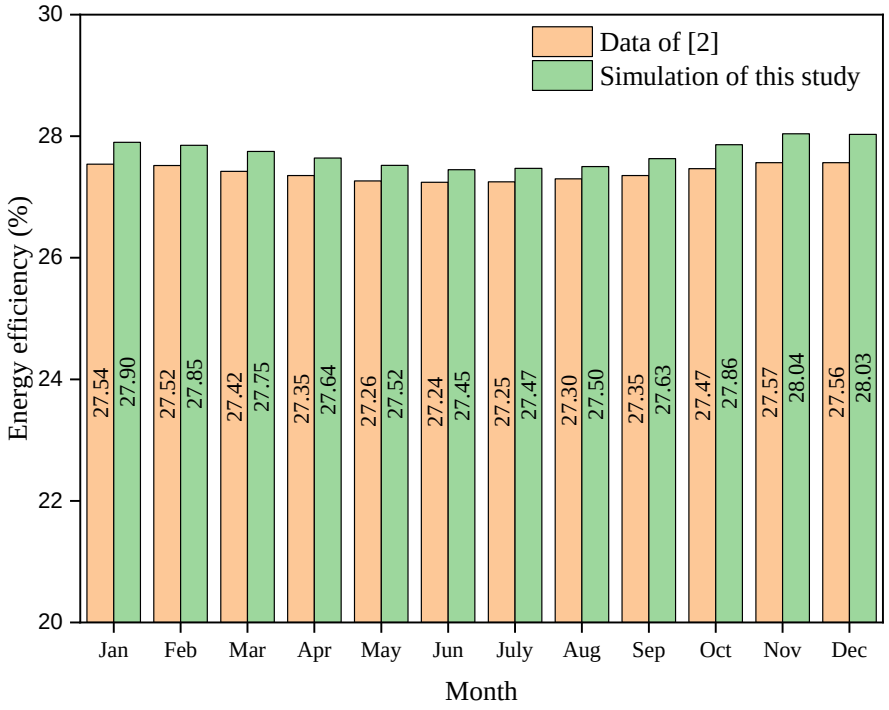

Figure 2. Validation of the present simulation framework against the data of Ref. [2].

3.2. Effect of price inflation on the optimal design

We first consider the effect of inflation on the decision variables, namely the solar collector area and the mass flow rate of the extracted ground water.

3.2.1. Solar collector area

Figure 3 shows that as inflation rises, the solar collector area required for the optimal design rises as well. For example, an inflation of 0.05 gives a solar collector area of 19815.0 m^2 but this increases by 8.42% to 21484.5 m^2 when inflation doubles to 0.10. A further rise in inflation to 0.15 leads to a further increase of 3.64% in the solar collector area. Therefore, the rate of change of the optimum solar collector area decreases with rising inflation. The solar collector area itself seems to follow a power-law relationship with rising inflation.

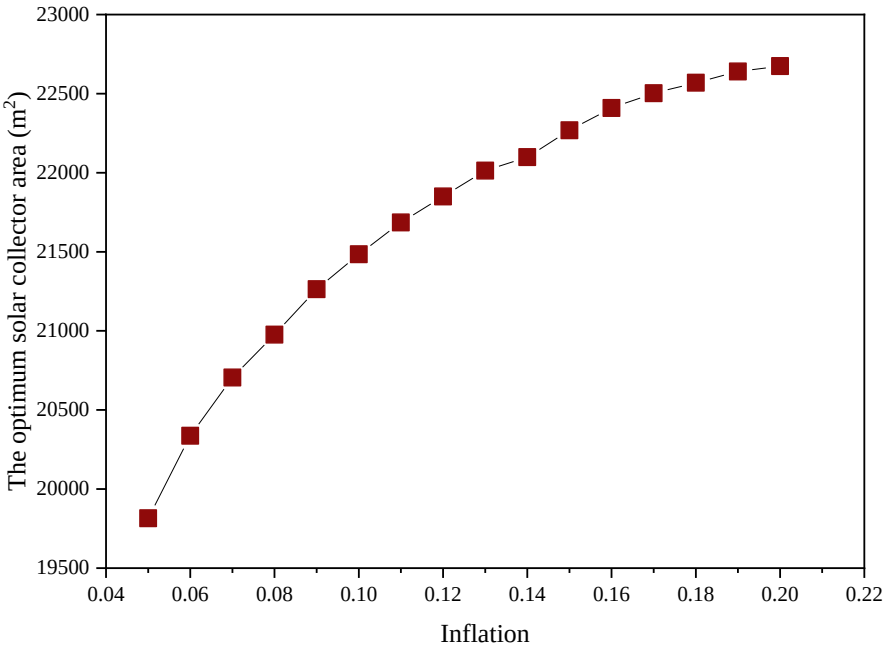

Figure 3. Effect of inflation on the optimum solar collector area.

3.2.2. Mass flow rate of the extracted ground water

Figure 4 shows that there is a downward trend in the extracted ground water mass flow rate as inflation rises. When inflation is 0.05, the system extracts 10.324 $kg.s^{-1}$ of ground water, but this drops to 8.251 $kg.s^{-1}$ when inflation rises to 0.20.

The costs of solar collectors are incurred only at the beginning, as an initial investment. The costs of using the ground water and its driving force, however, are distributed throughout the entire lifespan of the system. These costs therefore increase with rising inflation. As a result, the optimization algorithm prefers to provide more of the energy required to run the system via solar collectors, so that it is less exposed to the costs of rising inflation. This explains the opposing trends found in Figure 3 and Figure 4.

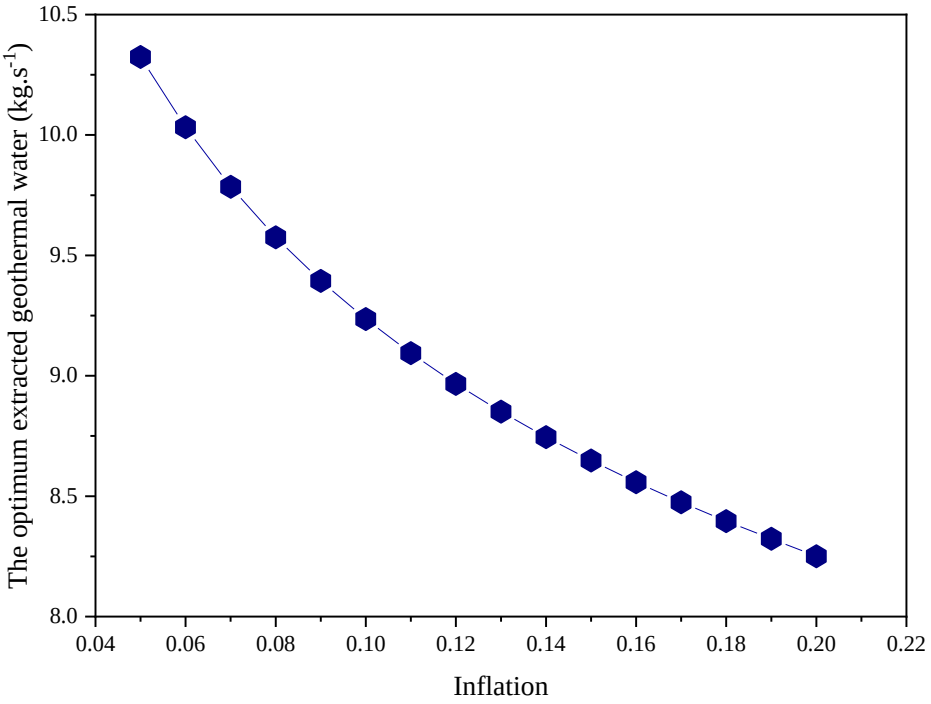

Figure 4. Effect of inflation on the optimum extracted ground water mass flow rate.

3.3. Effect of price inflation on the optimal performance

We now examine the effect of inflation on the objective functions, namely the annual production of H_2, water, power, and heat.

3.3.1. Annual H_2 production

The more solar radiation the system receives, the more hydrogen it can produce. Therefore, in the hotter months of the year, when the solar radiation is high, the system produces more hydrogen. Figure 5 shows that the annual H_2 production starts at 211.8 ton when inflation is 0.05, but then increases to 232.7 ton when inflation climbs to 0.20, a jump of nearly 10%. The H_2 production curve seems to follow a power-law scaling.

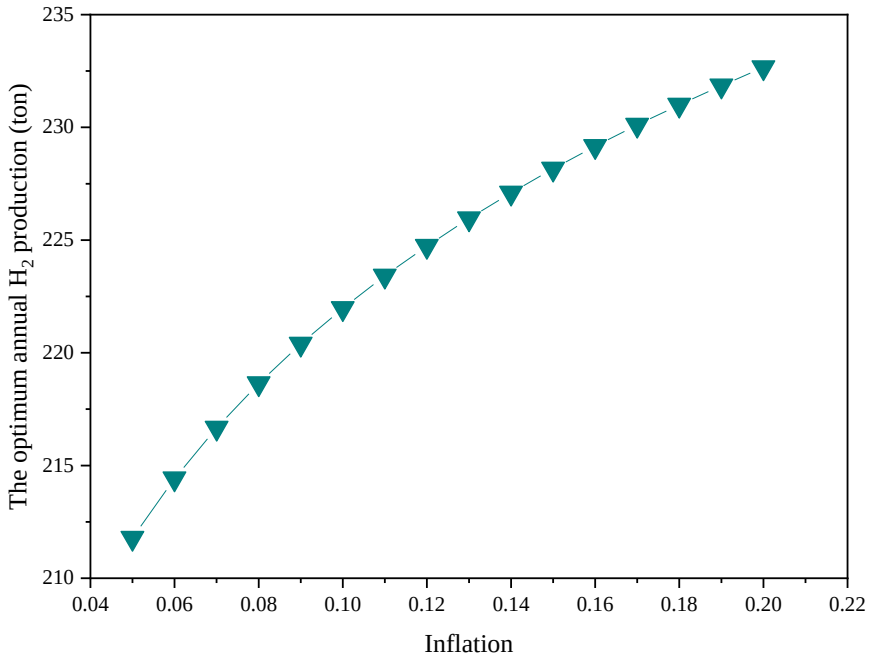

Figure 5. Effect of inflation on the optimum annual H_2 production.

3.3.2. Annual freshwater production

Unlike hydrogen production, the other system products are proportional to the change in the extracted ground water. Regarding the annual freshwater production, Figure 6 shows that the amount of water produced decreases with rising inflation in accordance with a polynomial function. When inflation is 0.05, the system generates 107387.5 tons of freshwater, but this drops

by 15.00% to 91270.3 ton when inflation rises fourfold to 0.20. This decrease is due to the part of the system that utilizes ground water to produce freshwater.

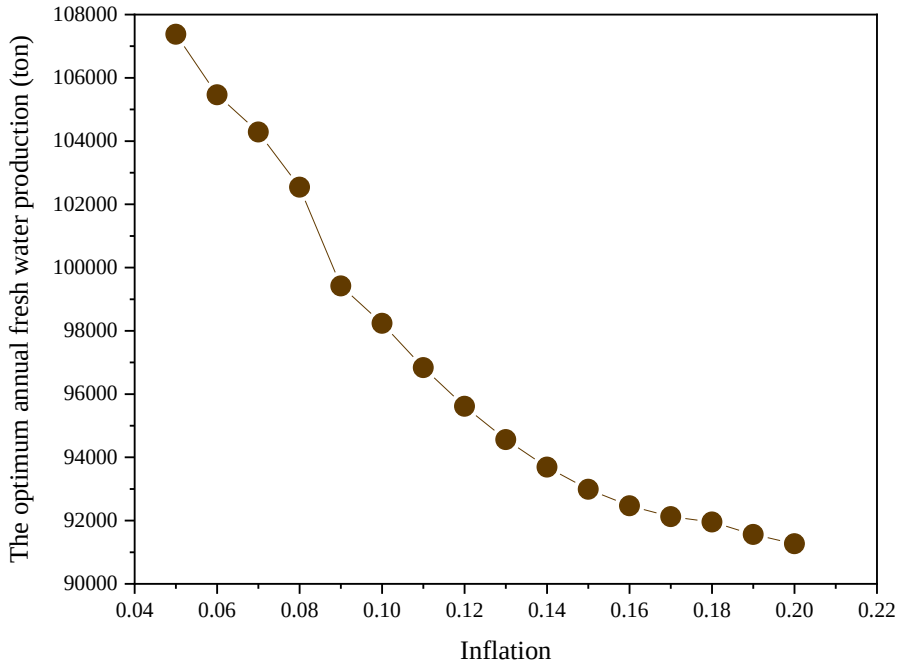

Figure 6. Effect of inflation on the optimum annual freshwater production.

3.3.3. Annual power production

Figure 7 shows that the optimum annual power production decreases with rising inflation. For initial inflation of 0.05, the system produces 304.3 MWh of power, but this drops by 37.3 MWh (or 12.25%) when inflation rises to 0.2. The rate of change of the power decreases with rising inflation, causing the power production itself to converge to 267.0 MWh. This trend is also due to the amount of extracted ground water, because the power is mainly produced by geothermal sources. The optimum annual power production seems to follow a polynomial function of degree 2.

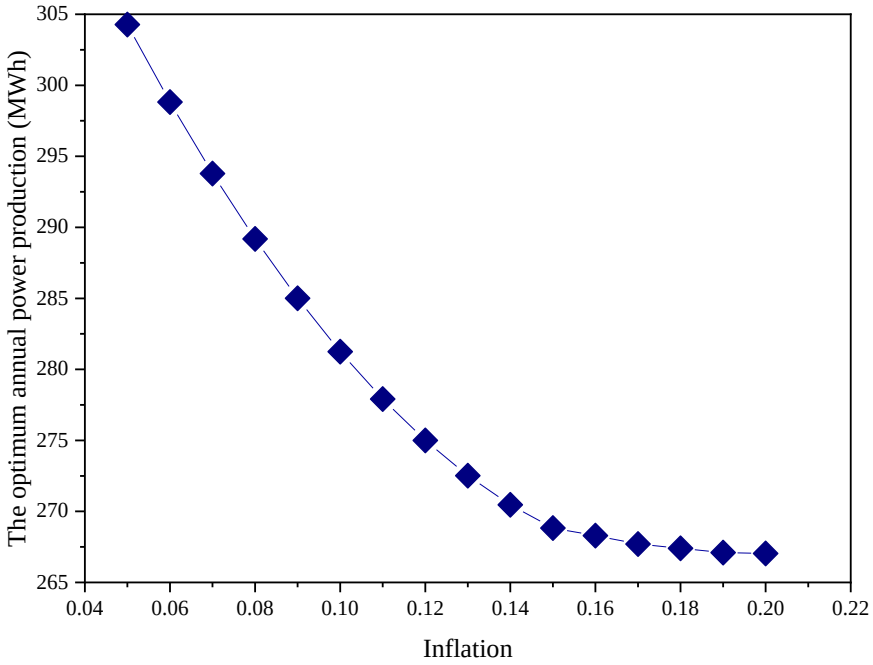

Figure 7. Effect of inflation on the optimum annual power production.

3.3.4. Annual heat production

The annual heat production follows a similar trend to that of the annual power production, as shown in Figure 8. This is because, like power generation, heat production is largely dependent on the geothermal part of the system and the extracted ground water. Furthermore, the change in heat production with rising inflation seems to exhibit polynomial behavior of degree 2. The system generates 2805.2 MWh of heat when inflation is 0.05, but this decreases by 11.95% to 2469.7 MWh when inflation rises to 0.20.

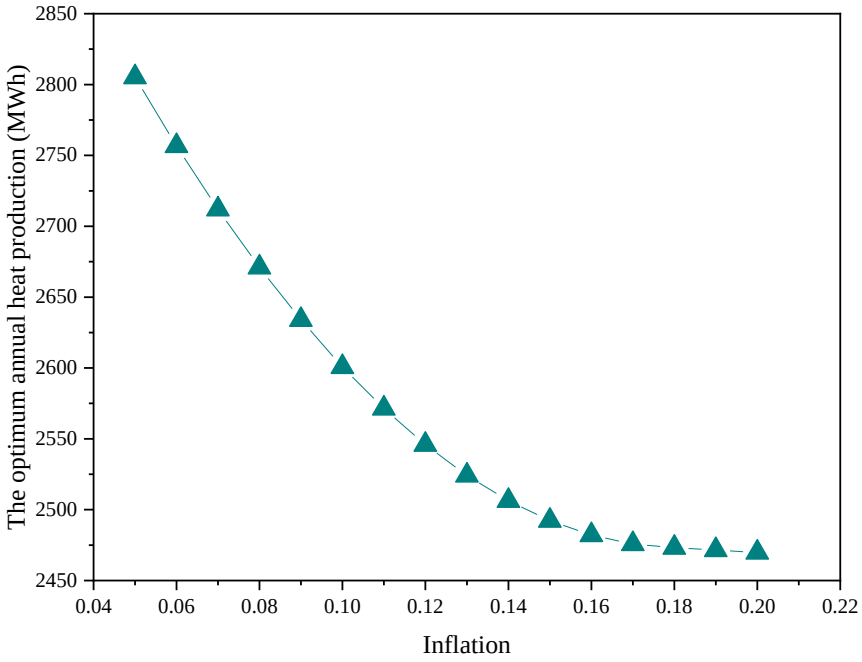

Figure 8. Effect of inflation on the optimum annual heat production.

3.4. Payback period

Figure 9 shows that the payback period increases with rising inflation, producing what seems to be a logarithmic trend. When inflation is 0.05, the payback period is 6.11 years, but this increases by 20.94% to 7.39 years when inflation rises to 0.20. This trend occurs because the diminishing effect of water, power, and heat production counterbalances the incremental effect of hydrogen production. Nevertheless, even when inflation is relatively high (0.20), the payback period is still reasonable, demonstrating the economic feasibility of the system design.

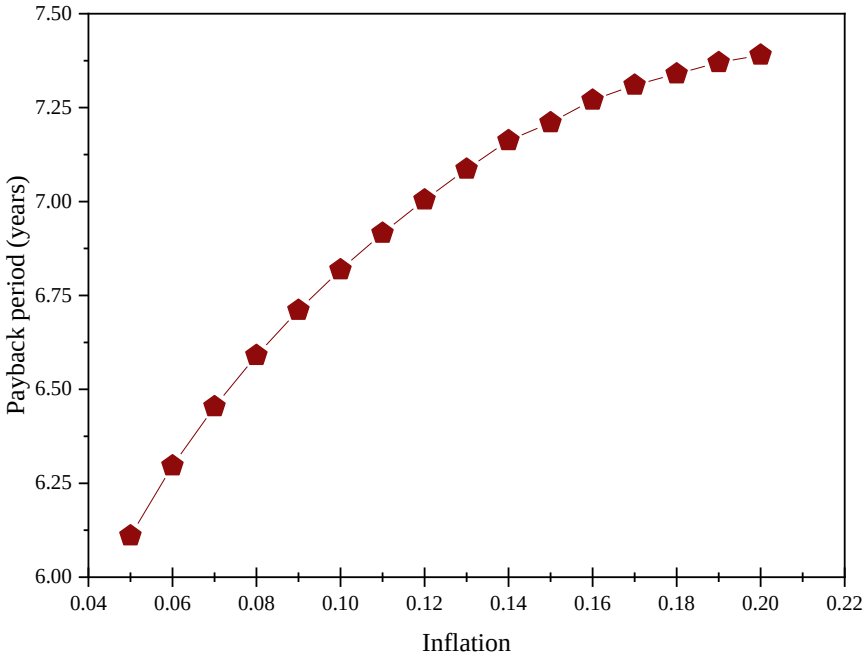

Figure 9. Effect of inflation on the optimum payback period.

4. Conclusions

We have shown that when inflation rises, an optimization algorithm combining NSGA-II and AHP tends to prefer balancing the system performance by increasing the solar collector area and decreasing the extracted mass flow rate of ground water. This preference arises because the solar collector area is paid for up front as an initial investment, so that it is not exposed to the effects of rising inflation, whereas the ground water becomes more expensive owing to payments distributed over the lifespan of the system. For this case study, we found that increasing inflation from 0.05 to 0.20 caused a 14.4% increase in solar collector area and a 20.1% decrease in the extracted mass flow rate of ground water.

The annual hydrogen production was found to be a function of the available solar collector area, which meant that it increased with rising inflation, whereas the other products (namely power, freshwater, and heat) decreased. The analysis also showed that as inflation rose from 0.05 to 0.20,

the annual hydrogen production increased by 9.9%, whereas the annual freshwater, power and heat production decreased by 15.0%, 12.2%, and 12.0%, respectively. The payback period also lengthened from 6.11 to 7.39 years, indicating that even at a relatively high inflation of 0.20, the payback period stayed within an acceptable range. This demonstrates the economic viability of simultaneously producing hydrogen, power, freshwater and heat via the present solar-geothermal system, even in times of rising inflation.

References

[1] Smil V. Energy and civilization: a history: MIT Press, 2018.
[2] Temiz M, Dincer I. Concentrated solar driven thermochemical hydrogen production plant with thermal energy storage and geothermal systems. Energy. 2021;219:119554.
[3] Karaca AE, Dincer I. An updated overview of Canada's hydrogen related research and development activities. International Journal of Hydrogen Energy. 2021;46(69):34515-25.
[4] Hoang AT, Huang Z, Nižetić S, Pandey A, Nguyen XP, Luque R, et al. Characteristics of hydrogen production from steam gasification of plant-originated lignocellulosic biomass and its prospects in Vietnam. International Journal of Hydrogen Energy. 2022;47(7):4394-425.
[5] IEA. World Energy Outlook 2021. 2021.
[6] UN. COP 26, Glasgow. 2021.
[7] Karayel GK, Javani N, Dincer I. Green hydrogen production potential for Turkey with solar energy. International Journal of Hydrogen Energy. 2021.
[8] Ozturk M, Dincer I. A comprehensive review on power-to-gas with hydrogen options for cleaner applications. International Journal of Hydrogen Energy. 2021;46(62):31511-22.
[9] Panwar N, Kaushik S, Kothari S. Role of renewable energy sources in environmental protection: A review. Renewable and sustainable energy reviews. 2011;15(3):1513-24.
[10] Rashwan SS, Dincer I, Mohany A. A review on the importance of operating conditions and process parameters in sonic hydrogen production. International Journal of Hydrogen Energy. 2021;46(56):28418-34.
[11] Gai L, Varbanov PS, Fan YV, Klemeš JJ, Nižetić S. Total Site Hydrogen Integration with fresh hydrogen of multiple quality and waste hydrogen recovery in refineries. International Journal of Hydrogen Energy. 2021.
[12] Karimi MH, Chitgar N, Emadi MA, Ahmadi P, Rosen MA. Performance assessment and optimization of a biomass-based solid oxide fuel cell and micro gas turbine system integrated with an organic Rankine cycle. International Journal of Hydrogen Energy. 2020;45(11):6262-77.
[13] Matulić N, Radica G, Barbir F, Nižetić S. Commercial vehicle auxiliary loads powered by PEM fuel cell. International Journal of Hydrogen Energy. 2019;44(20):10082-90.
[14] Penga Ž, Radica G, Barbir F, Nižetić S. Coolant induced variable temperature flow field for improved performance of proton exchange membrane fuel cells. International Journal of Hydrogen Energy. 2019;44(20):10102-19.
[15] Owusu PA, Asumadu-Sarkodie S. A review of renewable energy sources, sustainability issues and climate change mitigation. Cogent Engineering. 2016;3(1):1167990.
[16] Serra LM, Lozano M-A, Ramos J, Ensinas AV, Nebra SA. Polygeneration and efficient use of natural resources. Energy. 2009;34(5):575-86.

[17] Bui VG, Bui TMT, Hoang AT, Nižetić S, Nguyen Thi TX, Vo AV. Hydrogen-Enriched Biogas Premixed Charge Combustion and Emissions in Direct Injection and Indirect Injection Diesel Dual Fueled Engines: A Comparative Study. Journal of Energy Resources Technology. 2021;143(12).
[18] Sen O, Guler OF, Yilmaz C, Kanoglu M. Thermodynamic modeling and analysis of a solar and geothermal assisted multi-generation energy system. Energy Conversion and Management. 2021;239:114186.
[19] Kurşun B. Energy and exergy analysis of a concentrated photovoltaic recuperator design for a geothermal based multi-generation system. Applied Thermal Engineering. 2020;181:115932.
[20] Siddiqui O, Ishaq H, Dincer I. A novel solar and geothermal-based trigeneration system for electricity generation, hydrogen production and cooling. Energy Conversion and Management. 2019;198:111812.
[21] Chitgar N, Moghimi M. Design and evaluation of a novel multi-generation system based on SOFC-GT for electricity, fresh water and hydrogen production. Energy. 2020;197:117162.
[22] Ebrahimi-Moghadam A, Farzaneh-Gord M. Optimal operation of a multi-generation district energy hub based on electrical, heating, and cooling demands and hydrogen production. Applied Energy. 2022;309:118453.
[23] Alirahmi SM, Assareh E, Pourghassab NN, Delpisheh M, Barelli L, Baldinelli A. Green hydrogen & electricity production via geothermal-driven multi-generation system: Thermodynamic modeling and optimization. Fuel. 2022;308:122049.
[24] Alirahmi SM, Dabbagh SR, Ahmadi P, Wongwises S. Multi-objective design optimization of a multi-generation energy system based on geothermal and solar energy. Energy Conversion and Management. 2020;205:112426.
[25] Behzadi A, Habibollahzade A, Ahmadi P, Gholamian E, Houshfar E. Multi-objective design optimization of a solar based system for electricity, cooling, and hydrogen production. Energy. 2019;169:696-709.
[26] Colakoglu M, Durmayaz A. Energy, exergy and economic analyses and multiobjective optimization of a novel solar multi-generation system for production of green hydrogen and other utilities. International Journal of Hydrogen Energy. 2022.
[27] Mostafaeipour A, Rezaei M, Moftakharzadeh A, Qolipour M, Salimi M. Evaluation of hydrogen production by wind energy for agricultural and industrial sectors. International Journal of Hydrogen Energy. 2019;44(16):7983-95.
[28] Jahangiri M, Shamsabadi AA, Mostafaeipour A, Rezaei M, Yousefi Y, Pomares LM. Using fuzzy MCDM technique to find the best location in Qatar for exploiting wind and solar energy to generate hydrogen and electricity. International Journal of Hydrogen Energy. 2020;45(27):13862-75.
[29] Almutairi K, Mostafaeipour A, Jahanshahi E, Jooyandeh E, Himri Y, Jahangiri M, et al. Ranking locations for hydrogen production using hybrid wind-solar: A Case Study. Sustainability. 2021;13(8):4524.
[30] Mostafaeipour A, Rezayat H, Rezaei M. A thorough investigation of solar-powered hydrogen potential and accurate location planning for big cities: A case study. International Journal of Hydrogen Energy. 2020;45(56):31599-611.
[31] Messaoudi D, Settou N, Negrou B, Rahmouni S, Settou B, Mayou I. Site selection methodology for the wind-powered hydrogen refueling station based on AHP-GIS in Adrar, Algeria. Energy Procedia. 2019;162:67-76.
[32] Wu Y, Deng Z, Tao Y, Wang L, Liu F, Zhou J. Site selection decision framework for photovoltaic hydrogen production project using BWM-CRITIC-MABAC: A case study in Zhangjiakou. Journal of Cleaner Production. 2021;324:129233.
[33] Li J, Zoghi M, Zhao L. Thermo-economic assessment and optimization of a geothermal-driven tri-generation system for power, cooling, and hydrogen production. Energy. 2022:123151.
[34] Shaofu M, Hani EHB, Tao H, Xu Q. Exergy, economic, and optimization of a clean hydrogen production system using waste heat of a steel production factory. International Journal of Hydrogen Energy. 2021.

[35] Safari F, Dincer I. Assessment and multi-objective optimization of a vanadium-chlorine thermochemical cycle integrated with algal biomass gasification for hydrogen and power production. Energy Conversion and Management. 2022;253:115132.
[36] Farsi A, Dincer I, Naterer GF. Exergo- economic assessment by a specific exergy costing method for an experimental thermochemical hydrogen production system. International Journal of Energy Research. 2021;45(12):17358-77.
[37] Ansari SA, Kazim M, Khaliq MA, Abdul Hussain Ratlamwala T. Thermal analysis of multigeneration system using geothermal energy as its main power source. International Journal of Hydrogen Energy. 2021;46(6):4724-38.
[38] Mahmoudan A, Esmaeilion F, Hoseinzadeh S, Soltani M, Ahmadi P, Rosen M. A geothermal and solar-based multigeneration system integrated with a TEG unit: Development, 3E analyses, and multi-objective optimization. Applied Energy. 2022;308:118399.
[39] Sohani A, Delfani F, Hosseini M, Sayyaadi H, Karimi N, K.B. Li L, et al. Dynamic Multi-Objective Optimization Applied to a Solar-Geothermal MultiGeneration System for Hydrogen Production, Desalination, and Energy Storage (In press). International Journal of Hydrogen Energy. 2022.
[40] Sohani A, Sayyaadi H. End-users' and policymakers' impacts on optimal characteristics of a dew-point cooler. Applied Thermal Engineering. 2020;165:114575.
[41] Sohani A, Delfani F, Fassadi Chimeh A, Hoseinzadeh S, Panchal H. A conceptual optimum design for a high-efficiency solar-assisted desalination system based on economic, exergy, energy, and environmental (4E) criteria. Sustainable Energy Technologies and Assessments. 2022;52:102053.
[42] Sohani A, Dehnavi A, Sayyaadi H, Hoseinzadeh S, Goodarzi E, Garcia DA, et al. The real-time dynamic multi-objective optimization of a building integrated photovoltaic thermal (BIPV/T) system enhanced by phase change materials. Journal of Energy Storage. 2022;46:103777.
[43] Sohani A, Naderi S, Torabi F. Comprehensive comparative evaluation of different possible optimization scenarios for a polymer electrolyte membrane fuel cell. Energy Conversion and Management. 2019;191:247-60.
[44] Saaty TL. A scaling method for priorities in hierarchical structures. Journal of Mathematical Psychology. 1977;15(3):234-81.
[45] Saaty TL. Decision making with the analytic hierarchy process. International journal of services sciences. 2008;1(1):83-98.

Declaration of interests

☒ The authors declare that they have no known competing financial interests or personal relationships that could have appeared to influence the work reported in this paper.

☐The authors declare the following financial interests/personal relationships which may be considered as potential competing interests: